Cancer Research

# Intracellular ATP Levels Are a Pivotal Determinant of Chemoresistance in Colon Cancer Cells

Yunfei Zhou[1], Federico Tozzi[1], Jinyu Chen[3], Fan Fan[1], Ling Xia[1], Jinrong Wang[3], Guang Gao[3], Aijun Zhang[4], Xuefeng Xia[4], Heather Brasher[3], William Widger[3], Lee M. Ellis[1,2], and Zhang Weihua[3]

## Abstract

Altered metabolism in cancer cells is suspected to contribute to chemoresistance, but the precise mechanisms are unclear. Here, we show that intracellular ATP levels are a core determinant in the development of acquired cross-drug resistance of human colon cancer cells that harbor different genetic backgrounds. Drug-resistant cells were characterized by defective mitochondrial ATP production, elevated aerobic glycolysis, higher absolute levels of intracellular ATP, and enhanced HIF-1α–mediated signaling. Interestingly, direct delivery of ATP into cross-chemoresistant cells destabilized HIF-1α and inhibited glycolysis. Thus, drug-resistant cells exhibit a greater "ATP debt" defined as the extra amount of ATP needed to maintain homeostasis of survival pathways under genotoxic stress. Direct delivery of ATP was sufficient to render drug-sensitive cells drug resistant. Conversely, depleting ATP by cell treatment with an inhibitor of glycolysis, 3-bromopyruvate, was sufficient to sensitize cells cross-resistant to multiple chemotherapeutic drugs. In revealing that intracellular ATP levels are a core determinant of chemoresistance in colon cancer cells, our findings may offer a foundation for new improvements to colon cancer treatment. *Cancer Res; 72(1); 304–14. ©2011 AACR.*

## Introduction

Acquired chemoresistance is one of the major challenges in patients with advanced stage malignancies. Studies have revealed genetic and epigenetic alterations that cancer cells acquire to adapt to chemotherapeutic stress for survival purposes. Such alterations include increases in drug efflux, enhanced drug inactivation, enhanced DNA damage repair, mutations of survival-related genes, deregulated growth factor signaling pathways, increases in antiapoptotic gene expressions, and activation of intracellular survival signaling. Different types of cancer cells may depend more or less on some of these survival mechanisms (1). Advances are being made in identifying gene signatures that may predict drug-specific resistance prior to chemotherapy (2, 3). However, cancers that are resistant to one type of chemotherapeutic are often resistant to other chemotherapeutics, which is often referred to as cross-resistance, ultimately leads to treatment failure in nearly all patients with metastatic disease (4). The phenomenon of cross-resistance indicates that there might be a more centralized mechanism that cancer cells use to resist chemotherapeutic stresses.

Cell death can be executed by different mechanisms, including apoptosis, autophagy, necrosis, or combinations of these processes. Although different cell death mechanisms are unique in their molecular signaling cascades, one molecule is involved in the processes that mediate all types of cell death, ATP. During late-stage apoptosis, ATP levels sharply drop, mostly because of the loss of mitochondrial function and consumption by ATP-dependent proteases. In autophagy, a rescue process of self-degradation to compensate for energy paucity is also featured with ATP insufficiency prior to cell death (5, 6). During necrosis, depletion of ATP precedes mitochondrial permeability changes (7). The fact that ATP deprivation occurs in all types of cell death suggests that energy metabolism may play a critical role in the survival of cancer cells under stress.

Altered energy metabolism, such as enhanced aerobic glycolysis, is not only one of the fundamental phenotypes of malignant tumors but also plays important roles during tumor progression, metastasis, and relapse (8–10). The role of metabolic alterations of cancer cells in the development of acquired chemoresistance remains to be elucidated.

In this study, we developed cross-chemoresistant human colon cancer cell lines of different genetic backgrounds, HT29

**Authors' Affiliations:** Departments of [1]Cancer Biology and [2]Surgical Oncology, The University of Texas MD Anderson Cancer Center; [3]Department of Biology and Biochemistry, Center for Nuclear Receptors and Cell Signaling, University of Houston; and [4]Diabetic Research Center, Methodist Hospital Institute of Research, Houston, Texas

**Note:** Supplementary data for this article are available at Cancer Research Online (http://cancerres.aacrjournals.org/).

Y. Zhou and F. Tozzi contributed equally to this work.

**Corresponding Authors:** Zhang Weihua, Department of Biology and Biochemistry, Center for Nuclear Receptors and Cell Signaling, College of Natural Sciences and Mathematics, University of Houston, Science & Engineering Research Center Bldg 545, 3605 Cullen Blvd, Houston, TX 77204. Phone: 832-842-8811; Fax: 713-743-0634; E-mail: wzhang13@uh.edu and Lee M Ellis, Department of Cancer Biology, The University of Texas MD Anderson Cancer Center, 1515 Holcombe Blvd-173, Houston, TX 77230. Phone: 713-792-6926; Fax: 713-792-8747; E-mail: lellis@mdanderson.org

**doi:** 10.1158/0008-5472.CAN-11-1674

(mutated *BRAF* and *P53*, microsatellite stable) and HCT116 (mutated *KRAS* and *PIK3CA*, microsatellite unstable; ref. 11), by long-term culturing of cells in the presence of chemotherapeutic agent, oxaliplatin. We compared the glucose metabolism of drug-resistant cells with that of their parental cells and investigated the role of absolute level of intracellular ATP in the development of drug resistance of these cells. We found that drug-resistant cells showed defective mitochondrial ATP production, enhanced aerobic glycolysis, higher intracellular ATP levels, and enhanced hypoxia-inducible factor-1 alpha (HIF-1α)–mediated signaling that was reverted by direct delivery of ATP into cells. Importantly, direct delivery of ATP into cells caused drug-sensitive parental cells to become drug resistant.

## Materials and Methods

### Cell lines and *in vitro* chemoresistant model

The human colon cancer cell lines HT29 and HCT116 were obtained from the American Type Culture Collection (ATCC). The oxaliplatin-resistant cell lines HT29-OxR and HCT116-OxR were developed in our laboratory as previously described (12). Briefly, cells stably resistant to oxaliplatin were developed by exposing parental HT29 and HCT116 cells to an initial oxaliplatin dose of 0.1 μmol/L and culturing surviving cells to a confluence of 80% for 3 passages (∼6 weeks). The cells that survived initial oxaliplatin treatment were then exposed to 0.5 μmol/L oxaliplatin for 3 passages (∼8 weeks) and then 1.0 μmol/L for 3 passages (∼8 weeks). Finally, the oxaliplatin concentration was increased to the clinically relevant plasma concentration of 2 μmol/L for 3 weeks (∼10 weeks). The surviving resistant cells were named HT29-OxR and HCT116-OxR. All cells were cultured in minimal essential medium containing 5 mmol/L glucose and supplemented with 10% fetal bovine serum, vitamins, nonessential amino acids, penicillin–streptomycin, sodium pyruvate, and L-glutamine (Life Technologies). Oxaliplatin-resistant cells were continuously cultured in 2 μmol/L oxaliplatin unless otherwise indicated. Cell viability was measured by a Vi-cell XR cell viability analyzer (Beckman Coulter). *In vitro* experiments were carried out at 70% cell confluence and confirmed in at least 3 independent experiments. All cell lines are authenticated by short tandem repeats sequencing and matched with 100% accuracy to the ATCC database.

### MTT assay for $IC_{50}$ determination

Cell growth inhibition was determined by MTT assay in 96-well plates. First, 1,500–3,000 cells per well per 100 μL were seeded in 96-well plates. On the same day, 100 μL working stock of drug solution of oxaliplatin or 5-fluorouracil (5-FU) with 2× concentration of the final concentration was added to the cell suspension. After 72 hours drug incubation, 50 μL MTT reagent was added to each well and incubated for 4 hours. After the supernatant was removed, the formazan precipitates in the cells were dissolved in 200 μL dimethyl sulfoxide. Absorbance was determined by a MultiSkan plate reader (LabSystems) at 570 nm. Fractional survival was plotted against logarithm of drug dose, and $IC_{50}$ values were calculated by Prisms software (GraphPad Software). Oxaliplatin and 5-FU were purchased from the MD Anderson Cancer Center pharmacy. Both stock drugs were reconstituted in distilled water and maintained at room temperature.

### Measurement of cellular ATP, ADP, and AMP

Relative cellular ATP content was measured by the ATP-based CellTiter-Glo Luminescent Cell Viability kit (Promega) with modifications from the manufacturer's protocol. Briefly, cells were plated in 24-well plates at 20,000 cells per well to allow for attachment overnight. At the desired harvest time, an equal volume of the single-one-step reagent provided by the kit was added to each well and rocked for 15 minutes at room temperature. Cellular ATP content was measured by a luminescent plate reader. An additional plate with the same setup was used for cell counting by hemocytometer to normalize the cell number for calculating ATP level. The absolute amounts of cellular ATP, ADP, and AMP content were measured by the high-performance liquid chromatography coupled mass spectrum (HPLC-MS) method. Briefly, exponentially growing cells were trypsinized and washed with 2.5% glycerol (v/v) once. Cell pellets were frozen immediately in 100% ethanol with dry ice. Cell pellets were resuspended in 1 mL distilled water for ultrasonic fragmentation to release cellular ATP, ADP, and AMP. After centrifugation at 15,000 rpm for 5 minutes, the supernatant portions were collected to inject into the HPLC-MS machine for measurement of ATP, ADP, and AMP with the standard protocol. The total cellular ATP, ADP, and AMP amount was normalized by cell number.

### Spectrophotometric assay for phosphofructose kinase activity

Phosphofructose kinase (PFK) activity was determined as described previously (13) in an assay mixture containing 50 mm Tris-HCl (pH 8.0), 50 mmol/L KCl, 5 mm $MgCl_2$, 10 mm $(NH_4)_2SO_4$, 5 mmol/L dithiothreitol, 10 mmol/L fructose 6-phosphate, 0.28 mmol/L NADH, 3 units/mL aldolase, 30 units/mL triosephosphate isomerase, 10 units/mL α-glycerophosphate dehydrogenase, and cell lysate containing 50 μg/mL total protein in a final volume of 100 μL. The cell lysate was incubated with coupling enzymes at 37°C for 10 minutes. The reaction was started by the addition of NADH and fructose-6-phosphate, and NADH oxidation was followed by measuring the decrease in absorbance at 340 nm measured by a microplate reader at 37°C. Blank controls not containing the cell lysate were used to control nonspecific NADH oxidation. The reaction curves represent the average of triplicate results.

### In-plate measurement of mitochondrial oxygen consumption

Oxygen consumption rates (OCR) and extracellular acidification rates (ECAR) were measured by a Seahorse XF 24 analyzer (Seahorse Bioscience). Briefly, cells were seeded in 24-well cell culture microplates according to their growth rate and allowed to attach overnight. Approximately 30 minutes prior to the assay, culture medium was changed to unruffled Seahorse assay medium, and OCR/ECAR measurement was taken by the instrument every 10 minutes up to 2 hours. An average of quadruplicate readings for one cell line was

recorded and normalized by the number of cells, which were counted afterward using a Vi-cell XR cell viability analyzer (Beckman Coulter).

### Transmission electron microscopy

Parental and drug-resistant cells were plated in 6-well plates according to their growth rate and cultured to 70% confluency, at which time the cells were fixed with a solution containing 3% glutaraldehyde plus 2% paraformaldehyde in 0.1 mol/L cocodlate buffer, pH 7.3, for 1 hour. After fixation, the samples were submitted to the high-resolution electron microscopy facility at MD Anderson Cancer Center for processing using a JEM-1010 transmission electron microscope (JEOL USA, Inc.). Digital images were obtained by the AMT Imaging System (Advanced Microscopy Techniques). For each cell type, at least 20 individual cells were imaged and analyzed.

### Mitochondrial isolation and substrate ATP production

Mitochondrial ATP production was quantified by the ATP Bioluminescent Assay obtained from Sigma (FL-AA) with minor modifications to the manufacturer's protocol. ATP assay dilution buffer and ATP assay mix were prepared as directed using 40 μL of the ATP assay mix and 2 mL of the dilution buffer, aliquoted in advance, and stored at −80°C. The measurements were carried out by a white 96-well plate with a 100-μL total assay volume in each well. To each well, 41 μL of mitochondria (0.2–1.0 μg) and 4 μL of an electron transport substrate (either 500 mmol/L glutamate plus 500 mmol/L malate, or 500 mmol/L succinate) was added. To the mitochondrial substrate mixture, 5 μL of 100 μmol/L ADP was added to each reaction to initiate ATP production at time zero. The reaction was incubated between 30 and 45 seconds, followed by the addition of 50 μL of assay reaction mixture for bioluminescence measurements. Luminescence was recorded, in triplicate, using a Bio-Tek Instruments FLx-800 Fluorescent Microplate Reader equipped with KC4 BioTek software approximately 2 minutes after the addition of ADP (initial measurement), and measurements were continued for 10 minutes using the kinetic measurement mode at 1-minute intervals at a sensitivity level of 100. A 0 to 0.25 nmol/L ATP standard curve was generated by a standard solution of 10 μmol/L ATP. ATP stock concentration was determined at 259 nm with millimolar extinction coefficient for ATP ($E_{mM}$) = 15.4 $mmol/L^{-1}cm^{-1}$ (14). The value of ATP produced by mitochondria within 1 minute was normalized by the protein content of the mitochondria, which is expressed as "nmol ATP/min/mg protein."

### Measurement of cellular glycolytic activity

Glycolytic activity in the parental and resistant colon cancer cells was determined by measuring glucose consumption and lactate production. Cells were seeded in 6-well cell culture microplates at $0.5 \times 10^6$ to $1 \times 10^6$ cells per well per 3 mL according to their growth rate and allowed to attach overnight. Fresh medium was replaced the next morning approximately 3 hours prior to the assay. Cell culture medium was sampled at 200 μL at 3 time points at 3-hour intervals. The glucose and lactic acid concentrations of the cell culture medium were measured by a Dual-Channel Biochemistry Analyzer-2700D (YSI Life Sciences). For each time point, triplicate samples were measured to calculate the average values. Cell numbers were counted with a Beckman Coulter cell viability analyzer to normalize the glucose and lactic acid concentrations.

### Western blot and antibodies

The antibody against PARP was purchased from Cell Signaling. HIF-1α antibody was purchased from BD Transduction Laboratories. Glut-1 antibody was purchased from Abcam. β-actin, p21, and hexokinase II antibodies were purchased from Santa Cruz Biotechnology. VEGFA antibody was purchased from R&D Systems. Whole-cell lysate was collected from cells cultured at 70% confluency before Western blot analysis was applied. VEGF-A secretion into culture medium was examined using conditioned medium collected and analyzed by Western blot as previously described (15).

### Quantitative real-time PCR for VEGF-A

VEGF-A gene expression level in the parental and resistant cells was analyzed by quantitative real-time PCR using Taqman primers (Applied Biosystems) specific for the *VEGF-A* gene. Actin was used as an internal control. Total RNA was extracted from 60% to 70% confluent tumor cells growing in culture using TRIzol reagent (Life Technologies). Reverse transcription PCR was carried out by the First-Step RT-PCR Kit (Invitrogen). Real-time PCR reaction was carried out using PCR Master Mix (Roche) on ABI-7500 platform (Applied Biosystems).

### Liposome-encapsulated ATP delivery

Encapsulation of ATP into liposomes was carried out according to a published protocol (16). In brief, chloroform solution of phosphatidylcholine (0.26 mmol), cholesterol (0.12 mmol), and 1,2 dioleoyl-3-trimethyl-ammonium-propane (10.8 μmol) was evaporated, and the film formed was hydrated with/without 5 mL of 600 mmol/L ATP in Krebs-Henseleit (KH) buffer. The dispersion was frozen at −80°C for 30 minutes followed by thawing at 45°C for 5 minutes; this cycle was repeated 5 times. Nonencapsulated ATP was separated by dialysis against the KH buffer at 48°C overnight. For each treatment of cells with liposomes, 10 μL of either control or ATP liposomes were added into one well of a 6-well cell culture plate; the well contained 500 μL cell culture medium. Cells were harvested for analyses at indicated time points after liposome treatment.

## Results

### Characterization of chemoresistant phenotype of cross-resistant cell lines

Cells stably resistant to oxaliplatin were developed by exposing parental HT29 and HCT116 cells to increasing doses of oxaliplatin over successive passages as described in the Experimental Procedures section (12). The surviving resistant cell lines were named HT29-OxR and HCT116-OxR. The proliferation rates of both HT29-OxR and HCT116-OxR cells were slower than those of their parental cells, HT29 and HCT116 (Fig. 1A and Supplementary Table S1), consistent with an upregulation of cell-cycle regulator p21 (Supplementary Fig.

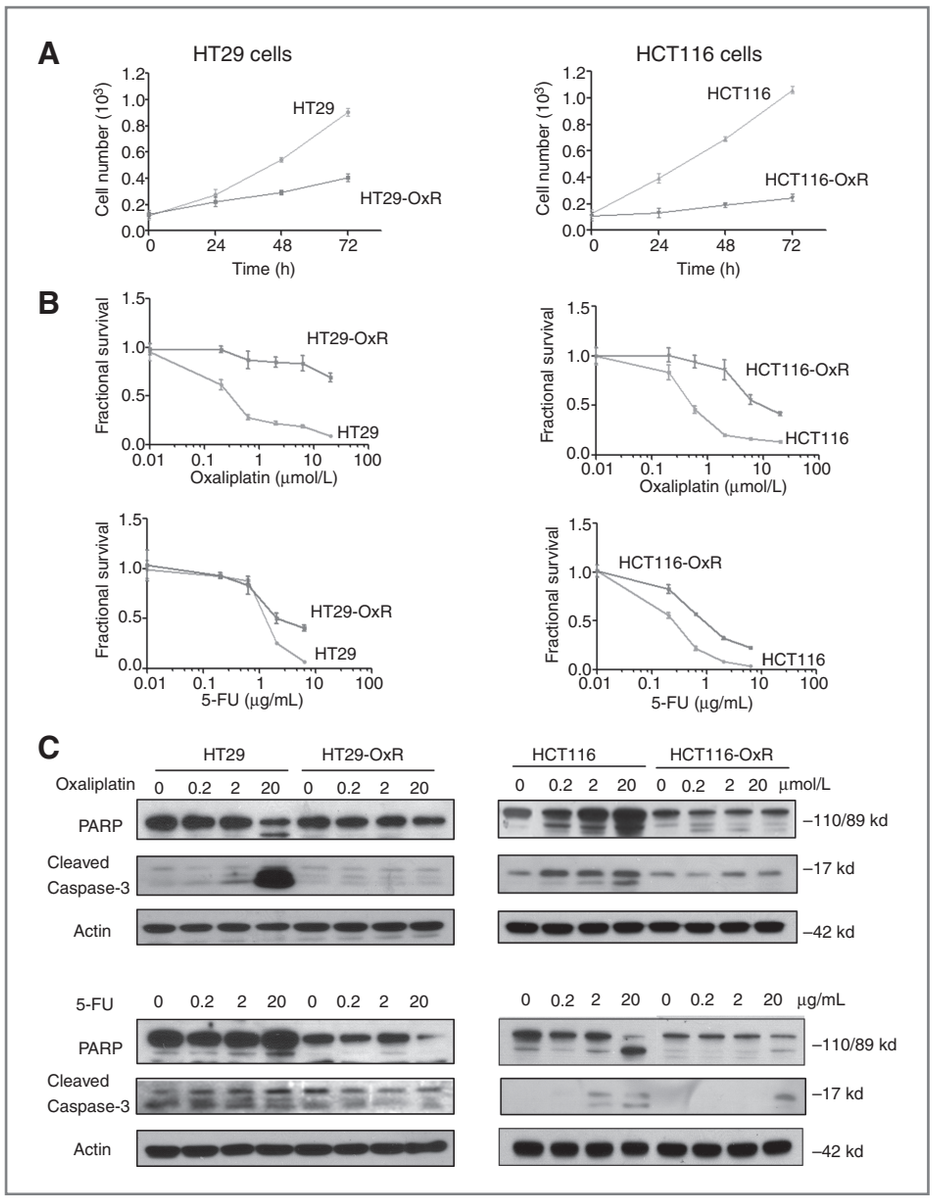


**Figure 1.** Characterization of cross-chemoresistant cancer cell lines. A, the drug-resistant cells were continuously maintained in media with 2 $\mu$mol/L oxaliplatin. Before plating for each experiment, media without drug was used for 2 passages. HT29-OxR and HCT116-OxR cells grew more slowly than their parental cells. See also Supplementary Table S1. B, survival inhibition curves from MTT assays showed a chemoresistant phenotype of HT29-OxR and HCT116-OxR cells to oxaliplatin (top) and 5-FU (bottom). C, HT29-OxR and HCT116-OxR showed decreased PARP cleavage (and thus decreased apoptosis) under 24-hour treatment with oxaliplatin (top) and 5-FU (bottom). Actin served as a loading control. All experiments were repeated at least 3 times. Representative data are shown.

S1). To confirm the chemoresistant phenotype after chronic oxaliplatin exposure, we compared the effect of oxaliplatin on HT29-OxR and HCT116-OxR cells to the effect on their parental cells by a 72-hour MTT assay (Fig. 1B). As expected, HT29-OxR and HCT116-OxR cells were more resistant to the cytotoxic effects of oxaliplatin compared with parental, chemonaïve cells.

To test the cross-chemoresistance of HT29-OxR and HCT116-OxR cells, we treated the resistant cells with 5-FU, a drug with a different mechanism of action from that of oxaliplatin, and observed cross-resistance of both cell lines to 5-FU. The chemoresistant phenotype was also reflected by more than 130- and 30-fold increases in the $IC_{50}$ to oxaliplatin in the HT29-OxR and HCT116-OxR cells, respectively, and 3- and 5-fold increases in the $IC_{50}$ to 5-FU (Table 1). Furthermore, exposure of both parental and resistant cells to increasing concentrations of oxaliplatin (0.2, 2, and 20 μmol/L) and 5-FU (0.2, 2, and 20 μg/mL) for 24 hours induced a concentration-dependent apoptotic event in the parental cells, but not in the resistant cells, as reflected by detection of PARP, caspase 3 cleavage by Western blot (Fig. 1C), and measurement of Annexin V–binding population by flow cytometry (Supplementary Fig. S2A and S2B). Thus, the stably selected HT29-OxR and HCT116-OxR cells display a phenotype of cross-chemoresistance to both oxaliplatin and 5-FU.

### Metabolic alterations and mitochondrial defects of chemoresistant cells

We hypothesized that under chronic exposure to genotoxic stressors, such as oxaliplatin and 5-FU, the surviving

**Table 1.** $IC_{50}$ values for oxaliplatin and 5-FU in parental (Par) and oxaliplatin-resistant colon cancer cells

| | HT29 | | | HCT116 | | |
|---|---|---|---|---|---|---|
| $IC_{50}$ | Par | OxR | O/P | Par | OxR | O/P |
| Oxal | 0.15 μmol/L | >20 μmol/L | >130 | 0.3 μmol/L | 9 μmol/L | 30 |
| 5-FU | 1 μg/mL | 3 μg/mL | 3 | 0.4 μg/mL | 2 μg/mL | 5 |

Abbreviation: O/P, ratio of OxR to parental cell values.

resistant cells will need to alter their energy metabolism to adapt to the continuous stress. Thus, we examined the cellular ATP levels of HT29-OxR, HCT116-OxR, and their respective parental cell lines using an ATP-based luminescent assay. Both resistant cell lines showed a 2-fold increase in total cellular ATP levels compared with their parental cells (Fig. 2A), indicating that a higher amount of ATP was produced in the resistant cells.

Cells produce ATP through 2 related mechanisms: glycolysis and mitochondrial oxidative phosphorylation. To determine which was involved in the chemoresistant cells, we measured the OCR by a Seahorse Bioenergizer (Seahorse Bioscience),

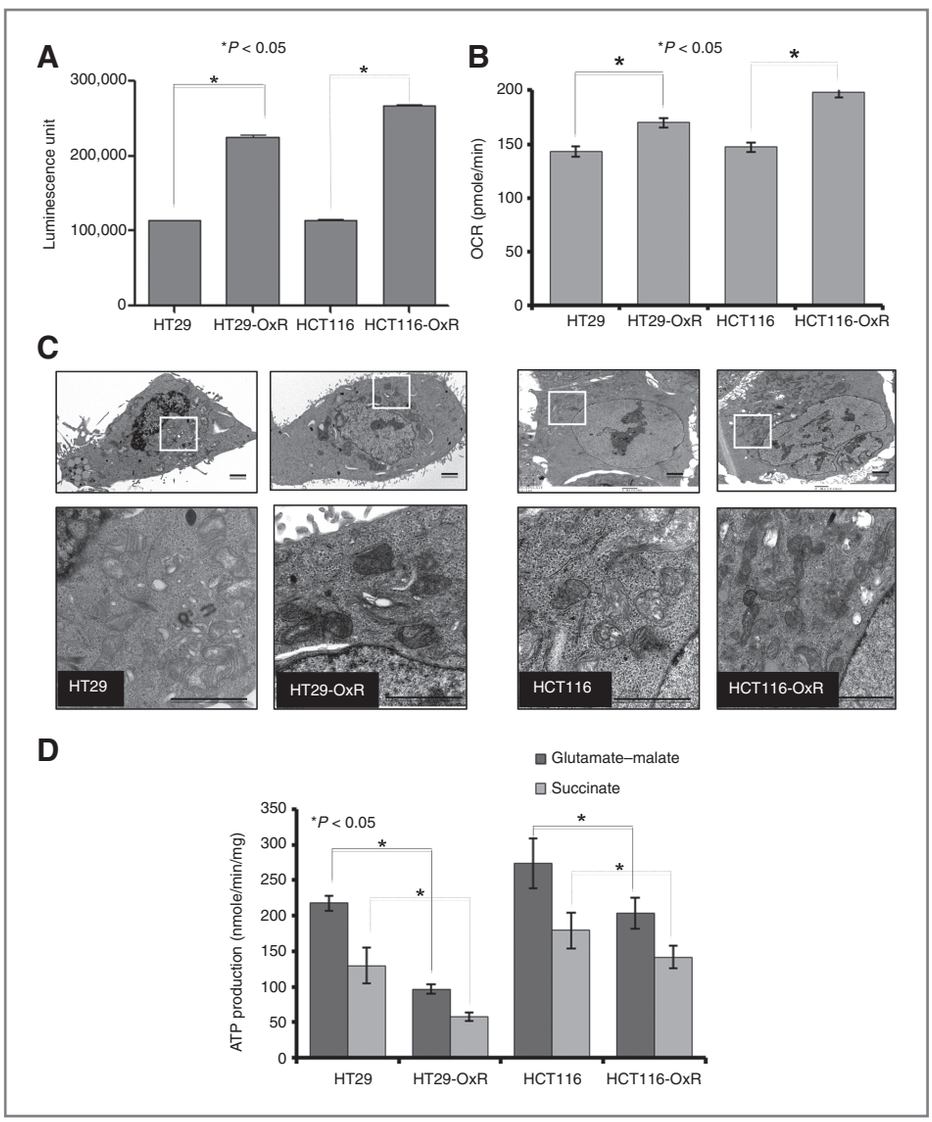


**Figure 2.** Measurement of intracellular ATP and mitochondrial activity. A, HT29-OxR and HCT116-OxR cells displayed more than a 2-fold increase in intracellular ATP levels compared with their parental cells. B, HT29-OxR and HCT116-OxR cells consumed oxygen at a significantly higher rate than their parental cells as indicated by OCR (pmole/min). C, HT29-OxR and HCT116-OxR cells displayed morphologic changes as examined by TEM. Bar, 2 μm. At least 20 individual cells were analyzed for each cell type. Representative images are shown. D, purified mitochondria from HT29-OxR and HCT116-OxR showed decreased substrate ATP production ability from both complex I (glutamate/malate as substrates) and complex II (succinate as a substrate) compared with that of their parental cells. All experiments were repeated at least 3 times. Representative data are shown.

which is often an indicator of mitochondrial oxidative phosphorylation activity (17). Interestingly, the HT29-OxR and HCT116-OxR cells exhibited a significantly elevated cellular OCR, suggesting the OxR cells may produce more ATP through upregulation of their mitochondrial oxidative phosphorylation (Fig. 2B).

To further determine changes in mitochondria, we examined the ultra-structure of mitochondria by transmission electronic microscopy (TEM). As shown in Fig. 2C, the TEM images showed 2 different patterns of alterations in the mitochondria of HT29-OxR and HCT116-OxR cells. The morphology of mitochondria of HT29-OxR is similar to the mitochondria of its parental cells; however, the mitochondria of HCT116-OxR cells are more elongated than that of its parental cells. A more condensed mitochondrial form was observed as a common feature in both resistant cell lines. The number of mitochondria in HT29-OxR cells did not change but increased in HCT116-OxR cells as compared with their parental cells, respectively (Supplementary Fig. S3).

The data showing enhanced oxygen consumption and the increased density of mitochondria in the resistant cells suggest that the mitochondria of these cells are more active, possibly for the purpose of generating more ATP. To test this, we measured the ATP-producing capacity of mitochondria isolated from the parental and resistant cells using complex-I substrates glutamate and malate and complex-II substrate succinate. Surprisingly, the mitochondria of resistant cells actually were significantly less capable of producing ATP than were their parental cells (Fig. 2D). In addition, the reserve mitochondrial oxidative phosphorylation capacity was significantly lower in the OxR cells after treatment with the uncoupler carbonilcyanide p-triflouromethoxyphenylhydrazone, as measured by the Seahorse Bioenergizer, suggesting defective mitochondrial function (Supplementary Fig. S4A). Taken together, these data suggest that the resistant cells used an alternative energy-producing mechanism to maintain a higher ATP levels.

### Elevated glycolysis of chemoresistant cells

To test whether the cross-chemoresistant cells also have altered aerobic glycolysis, we measured several key glycolytic parameters, including glucose consumption, lactate production, and expression levels of glycolytic enzymes in the resistant cells. As shown in Fig. 3A, both HT29-OxR and HCT116-OxR cells consumed more glucose than their parental cells. Accordingly, the resistant cells released more lactate into the media (Fig. 3B). Consistently, a comprehensive glycolytic parameter, ECAR, was significantly higher in the OxR cells compared with their parental cells, suggesting a higher glycolytic phenotype of the OxR cells (Supplementary Fig. S4B). In addition, the protein expression of glucose transporter (Glut-1) and hexokinase (HK2) were all significantly upregulated in HT29-OxR and HCT116-OxR cells (Fig. 3C).

A master regulator of glycolysis is HIF-1α (18), which is regulated by oxygen-dependent and oxygen-independent mechanisms (19). We next examined HIF-1α expression and found that HIF-1α was upregulated in both HT29-OxR and HCT116-OxR cells under normoxic conditions. To further prove a functional role of HIF-1α in the resistant cells, we examined the expression of *VEGF-A*, a known downstream gene of HIF-1α. We found several isoforms of VEGFA were increased in the HT29-OxR and HCT116-OxR conditioned media including the $VEGFA_{165}$ (Fig. 3D and Supplementary Fig. S5). Consistently, the mRNA levels of VEGFA were significantly upregulated in both resistant cell lines (Fig. 3D), suggesting a functional HIF1α pathway was elevated in the OxR cells.

### Intracellular ATP regulates HIF-1α and induces drug-resistant phenotype

The higher intracellular ATP level and defective mitochondrial ATP production in the chemoresistant cells as compared with the parental cells indicated that the resistant cells might need more ATP to survive under genotoxic stress. It is likely that the drug-resistant cells may turn to glycolysis for more rapid ATP generation. It is known that the ADP/AMP ratio determines the glycolytic rate through stereotypic regulation of the key glycolytic enzyme PFK and drives glycolysis (20). Therefore, we measured the levels of intracellular ADP and AMP using HPLC-MS. As shown in Fig. 4A, the ratio of ADP/AMP was much lower in HT29-OxR and HCT116-OxR cells than in their parental controls. We further measured the enzyme activity of PFK by a well-established *in vitro* biochemical assay (13) over a time course of 5 to 20 minutes using extracted cell lysates. In consistent with the decreased ADP/AMP ratio, the PFK enzyme activity was elevated in HT29-OxR cells and to a much higher level in HCT116-OxR cells as compared with their parental cells (Fig. 4B).

The activity of aerobic glycolysis, level of metabolic regulator HIF-1α, and cellular ATP level were higher in the resistant cells, which suggest that ATP has a protective role for cancer cells under genotoxic stress. To test this possibility, we artificially delivered ATP packaged in liposomal vehicles to the parental HT29 and HCT116 cells by transient transfection and examined the drug treatment effect on these cells. As shown in Fig. 4C, exogenous ATP supplementation partially blocked the cytotoxic effect of oxaliplatin in both cell lines, indicating the role of intracellular ATP level in mediating the drug-resistant phenotype.

We further hypothesized that the resistant cells are in need of more ATP; thus, a faster ATP production mechanism, namely, aerobic glycolysis, is elevated, which in turn demands a higher level of HIF-1α to enhance/sustain aerobic glycolysis (Fig. 3C). To test whether exogenous ATP delivery could affect HIF-1α level and glycolysis, we treated the resistant cells with ATP liposomes and examined the expression levels of HIF-1α and glycolytic enzymes. Consistent with our hypothesis, ATP treatment decreased HIF-1α rapidly in both HT29-OxR and HCT116-OxR cells, and reversed the glycolytic phenotype, as evidenced by a concordant decrease in hexokinase II expression in both resistant cell lines (Fig. 4D). The level of Glut-1 was not significantly altered at 2 hours ATP treatment, which is probably due to the protein turnover kinetics of Glut-1 being different from that of hexokinase II.

If the intracellular ATP level plays a central role in sustaining the survival of cross-chemoresistant cells, depletion of ATP

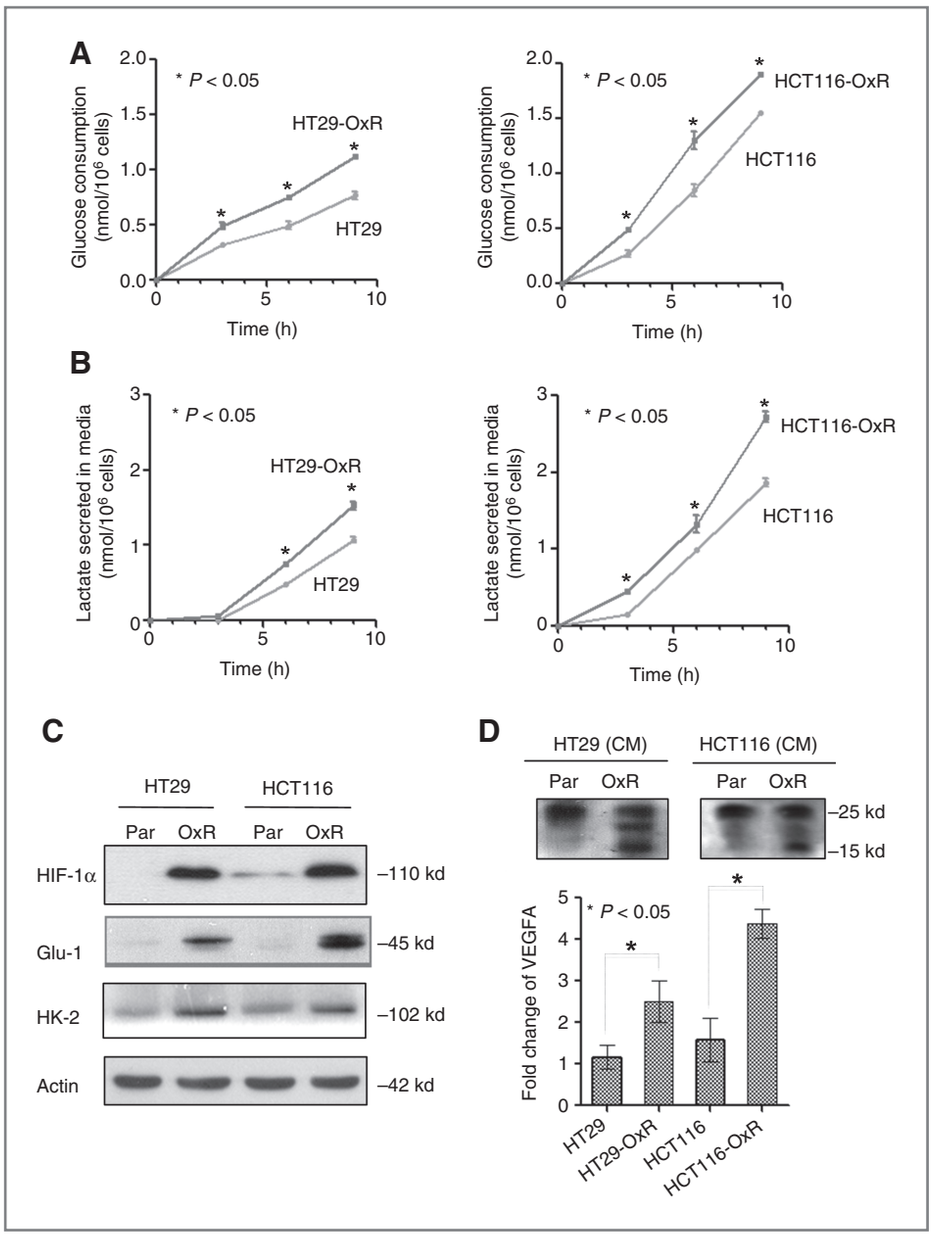


**Figure 3.** Characterization of glycolytic activity and HIF-1α activity. A, HT29-OxR and HCT116-OxR cells consumed glucose at a higher rate than their parental cells. B, HT29-OxR and HCT116-OxR cells produced lactate at a higher rate than their parental cells. C, key glycolytic enzymes GLUT1, HK2, LDHA, and HIF-1α were upregulated in HT29-OxR and HCT116-OxR cells compared with their parental (Par) cells, as shown by Western blot. D, HT29-OxR and HCT116-OxR produced more VEGFA into cell culture medium than their parental cells (top), which correlated with VEGFA mRNA level by quantitative PCR (bottom). All experiments were repeated at least 3 times. Representative data are shown.



should sensitize these cells to chemotherapeutic agents. As shown in Fig. 5A, 3-bromopyruvate (3-BrPA), a widely used ATP-depleting agent (21), depleted cellular ATP in HT29-OxR and HCT116-OxR cells in a dose-dependent manner. We pretreated the resistant cells with a moderate does of 3-BrPA (30 μmol/L) for 24 hours, then tested their sensitivity to oxaliplatin and 5-FU. As shown in Fig. 5B and C, ATP depletion partially reversed the drug-resistant phenotype and resensitized both resistant cell lines to oxaliplatin and 5-FU treatment. The $IC_{50}$ values of oxaliplatin and 5-FU in the OxR cells before and after ATP depletion by 3-BrPA treatment were calculated. There was a 2- to 3-fold decrease in the $IC_{50}$ in both OxR cell lines after ATP depletion (Supplementary Table S2). Taken together, our data suggest that intracellular ATP plays a central role in regulation of drug-resistant phenotype of colon cancer cells.

## Discussion

ATP, the energy currency of the cell, is produced from carbon fuels at 2 levels of metabolism, glycolysis in the cytosol and oxidative phosphorylation in the mitochondria. Glycolysis, besides producing pyruvate for oxidative phosphorylation under nonstressful conditions, generates 2 moles of ATP from 1 mole of glucose. In normal cells undergoing stress, for example, due to a sudden drop of intracellular ATP and hypoxia, cells will accelerate glycolysis to produce ATP to meet the immediate energy need; accelerated glycolysis leads to

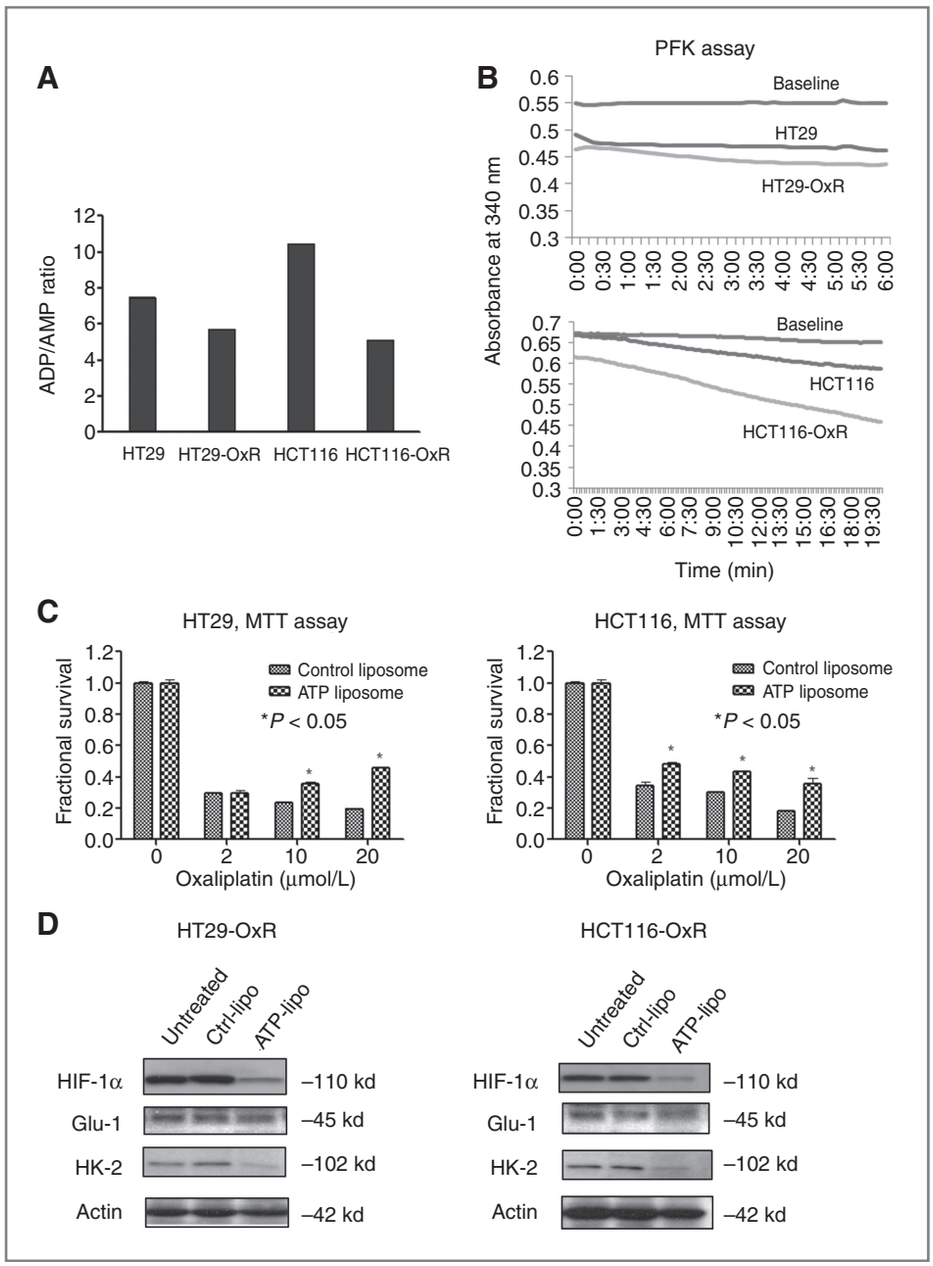


**Figure 4.** ATP regulates HIF-1$\alpha$ expression and induces a drug-resistant phenotype. A, ratio between absolute cellular ADP and AMP amount decreased in HT29-OxR and HCT116-OxR cells, as shown by HPLC-MS measurement. B, PFK enzyme activity is elevated in HT29-OxR and HCT116-OxR cells compared with parental cells. The enzyme activity is reflected by the decrease of absorbance at 340 nm (the *y* axis, unit) over the indicated time course (the *x* axis, minute; baseline, blank control). C, ATP liposomal delivery to parental HT29 and HCT116 cells induced resistance to oxaliplatin under 72-hour treatment, as shown by MTT assay. D, ATP liposomal delivery to HT29-OxR and HCT116-OxR cells decreased HIF-1$\alpha$ expression and reverted glycolytic enzyme HK2 expression. All experiments were repeated at least 3 times. Representative data are shown.

increased production of lactate from pyruvate (22, 23). Although the efficiency of ATP production via glycolysis is lower than that of oxidative phosphorylation, the ATP generation rate of glycolysis is nearly 100 times faster than that of oxidative phosphorylation. In tumors, elevated aerobic glycolysis differentiates malignant tumors from benign tumors and nontumor cells, a phenomenon that was identified by Otto Warburg (24) and has been repeatedly confirmed. One possible driver of the aerobic glycolysis of malignant tumor cells could be a higher ATP demand for the purposes of survival and growth as than demand in nonmalignant or normal cells (25). Our data support the hypothesis that metabolic shift driven by higher ATP demand is also applicable to the progression of acquired chemoresistance of cancer cells.

To cope with constant chemotherapeutic stress, chemoresistant cancer cells are known to do at least one of the following: increase drug efflux, enhance drug inactivation, enhance DNA damage repair, mutate survival-related genes, deregulate growth factor signaling pathways, increase expression of antiapoptotic genes, and/or activate intracellular survival signaling (1, 4). All of these activities consume ATP. Our data showing elevated aerobic glycolysis in the chemoresistant cells and sensitization of the chemoresistant cells by inhibition of glycolysis further argue that enhanced aerobic glycolysis of

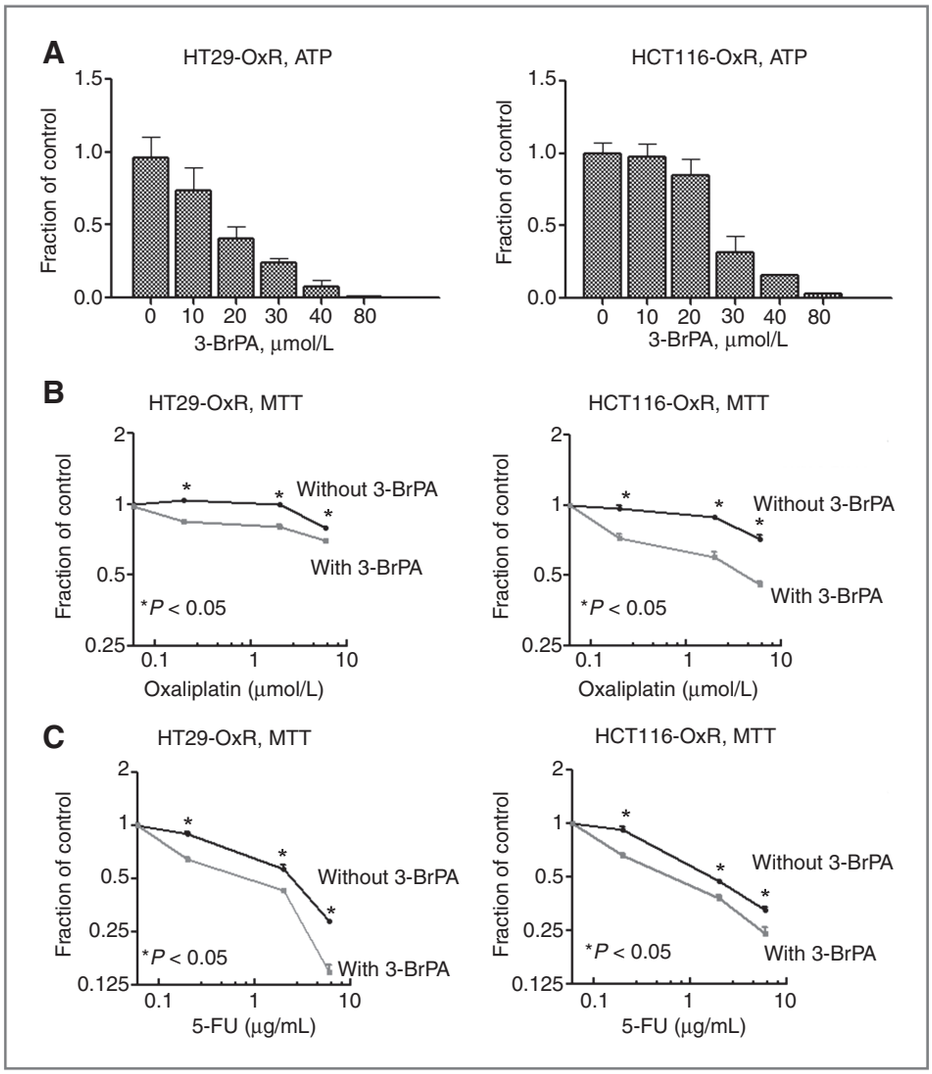


**Figure 5.** ATP depletion sensitizes drug-resistant cells to chemoreagent. A, 3-BrPA depleted cellular ATP level in HT29-OxR and HCT116-OxR cells after 24 hours of treatment, as measured by ATP luminescent activity. B, pretreatment of 3-BrPA (30 μmol/L) for 24 hours sensitized HT29-OxR and HCT116-OxR cells to oxaliplatin, as shown in 72-hour MTT assays. C, pretreatment of 3-BrPA (30 μmol/L) for 24 hours sensitized HT29-OxR and HCT116-OxR cells to 5-FU, as shown in 72-hour MTT assays. All experiments were repeated at least 3 times. Representative data are shown.

cancer cells occurs to provide the extra amount of ATP needed for chemoresistant cells to survive under stress. It is worth noting that the chemoresistant cells consume more oxygen while their mitochondrial ATP production is defective (Fig. 3D). Oxygen consumption has often been used as an indicator of mitochondrial ATP productivity. Our data support the argument that oxygen consumption is not a reliable index for mitochondrial ATP productivity (26). The role of enhanced oxygen consumption by chemoresistant cells warrants further investigation.

Extracellular ATP can be taken up by cells via adenosine transporters (27); however, because of signaling effects triggered by adenosine receptors (28), treating cells with naked ATP results in a complex of signaling responses besides an increase in the intracellular ATP level. Liposome-encapsulated ATP has been used to deliver ATP into cells *in vivo* (29–32), which allows us to avoid interfering with the signaling mediated by adenosine receptors. The comprehensive effects of delivering ATP directly into cells, reverting the aerobic glycolytic activity and HIF-1α level of cross-chemoresistant cells, and converting chemosensitive cells to resistant cells, further indicate that the chemoresistant cells are in need of more ATP.

In tumor tissues, upregulation of HIF-1α cannot be fully attributed to hypoxia. Increased expression of HIF-1α is often found in cancer cells of tissues in which oxygen supply is sufficient (33–35), and HIF-1α is upregulated only in the malignant tumor cells and not the benign tumor cells with the same tissue origin (36–39). For example, glucose deprivation induces HIF-1α expression in the presence of an ample amount of oxygen (40). Our finding of the oxygen-independent degradation of HIF-1α induced by the increase of intracellular ATP is novel. Although the molecular mechanism is currently under investigation, it bears important implications for cancer biology. The data suggest the possibility that insufficiency of intracellular ATP might be a driving force of oxygen-independent HIF-1α signaling in cancer cells, which in turn elevates aerobic glycolysis to produce ATP more efficiently to meet the increased demand of cancer cells. This possibility is supported by a recent finding that malignant tumor cells consume a

higher amount of ATP via the endoplasmic reticulum enzyme UDPase ENTPD5, that, in turn enhances aerobic glycolysis (41).

On the basis of the contradiction between a higher amount of ATP, HIF-1α, and glycolysis in chemoresistant cells and downregulation of HIF-1α and glycolysis by exogenous ATP delivery, and the chemoresistant effect of ATP on chemosensitive cells, we propose the concept of "ATP debt." ATP debt is the extra amount of ATP needed to maintain survival homeostatic pathways in cancer cells, which is equal to ATP needed for survival minus ATP produced. The decreased ADP/AMP ratio and increased PFK activity in the drug-resistant cells as compared with the parental cells indicates a higher ATP consumption rate in the drug-resistant cells. Thus, the drug-resistant cells demand a faster ATP generating mechanism to maintain survival, which is met by aerobic glycolysis/fermentation. Under these conditions, HIF-1α, as a key glycolysis regulator, is upregulated independent of oxygen levels. The steady-state higher level of HIF-1α in the drug-resistant cells and its downregulation by increased ATP levels suggests that more ATP is needed to cope with chemotherapeutic stress, that is, the drug-resistant cells have higher "ATP debt." The level of HIF-1α under normoxic conditions might be an indicator of ATP debt. Understanding the molecular mechanisms that cancer cells use to reduce their ATP debt may provide the foundation for the development of novel therapeutic strategies.

## Disclosure of Potential Conflicts of Interest

L.M. Ellis: consultant and advisory board, Genentech/Roche, Bristol-Myers Squibb. The other authors disclosed no potential conflicts of interest.

## Acknowledgments

The authors thank Kenneth Dunner Jr. and Robert Langley of the TEM core facility of MDACC for their assistance in mitochondrial morphology analysis; Edward Felix of the Pharmaceutical Development Center of MDACC for his assistance in HPLC-MS analysis of cellular ATP, ADP, and AMP content; Sunita Patterson (Department of Scientific Publications) for manuscript editing; and Rita Hernandez from the Departments of Surgical Oncology and Cancer Biology for editorial assistance.

## Grant Support

This work was supported in part by the NIH (UT MDACC Cancer Center Support grant CA016672), in part by the Texas Emerging Technology Fund No. 300-9-1958. F. Tozzi is supported by NIH T32 CA009599. Z. Weihua is supported by grants from the Center of Nuclear Receptors and Cell Signaling of University of Houston, American Cancer Society, and Congressional Directed Medical Research Programs of the Department of Defense. L.M. Ellis is supported by the William C. Liedtke, Jr. Chair in Cancer Research.

The costs of publication of this article were defrayed in part by the payment of page charges. This article must therefore be hereby marked *advertisement* in accordance with 18 U.S.C. Section 1734 solely to indicate this fact.

Received May 16, 2011; revised October 21, 2011; accepted October 28, 2011; published OnlineFirst November 14, 2011.

## References

1. Wilson TR, Longley DB, Johnston PG. Chemoresistance in solid tumours. Ann Oncol 2006;17 Suppl 10:x315–24.
2. Cree IA. Chemosensitivity and chemoresistance testing in ovarian cancer. Curr Opin Obstet Gynecol 2009;21:39–43.
3. Wan YW, Sabbagh E, Raese R, Qian Y, Luo D, Denvir J, et al. Hybrid models identified a 12-gene signature for lung cancer prognosis and chemoresponse prediction. PLoS One 2010;5:e12222.
4. Longley DB, Johnston PG. Molecular mechanisms of drug resistance. J Pathol 2005;205:275–92.
5. Lemasters JJ, Qian T, He L, Kim JS, Elmore SP, Cascio WE, et al. Role of mitochondrial inner membrane permeabilization in necrotic cell death, apoptosis, and autophagy. Antioxid Redox Signal 2002;4:769–81.
6. Skulachev VP. Bioenergetic aspects of apoptosis, necrosis and mitoptosis. Apoptosis 2006;11:473–85.
7. Vanlangenakker N, Vanden Berghe T, Krysko DV, Festjens N, Vandenabeele P. Molecular mechanisms and pathophysiology of necrotic cell death. Curr Mol Med 2008;8:207–20.
8. Ferreira LM. Cancer metabolism: the Warburg effect today. Exp Mol Pathol 2010;89:372–80.
9. Kaelin WG Jr., Thompson CB. Q&A: Cancer: clues from cell metabolism. Nature 2010;465:562–4.
10. Hanahan D, Weinberg RA. Hallmarks of cancer: the next generation. Cell 2011;144:646–74.
11. Jhawer M, Goel S, Wilson AJ, Montagna C, Ling YH, Byun DS, et al. PIK3CA mutation/PTEN expression status predicts response of colon cancer cells to the epidermal growth factor receptor inhibitor cetuximab. Cancer Res 2008;68:1953–61.
12. Yang AD, Fan F, Camp ER, van Buren G, Liu W, Somcio R, et al. Chronic oxaliplatin resistance induces epithelial-to-mesenchymal transition in colorectal cancer cell lines. Clin Cancer Res 2006;12:4147–53.
13. Kamemoto ES, Mansour TE. Phosphofructokinase in the liver fluke Fasciola hepatica. Purification and kinetic changes by phosphorylation. J Bio Chem 1986;261:4346–51.
14. Costa M, Shute B, Mergner WJ. Measurement of ATP synthesis and flocculent matrix densities in mitochondria as a function of '*in vitro*' ischemia in the heart and liver of rats. Pathobiology 1990;58:129–37.
15. Samuel S, Fan F, Dang LH, Xia L, Gaur P, Ellis LM. Intracrine vascular endothelial growth factor signaling in survival and chemoresistance of human colorectal cancer cells. Oncogene 2010;30:1205–12.
16. Verma DD, Levchenko TS, Bernstein EA, Torchilin VP. ATP-loaded liposomes effectively protect mechanical functions of the myocardium from global ischemia in an isolated rat heart model. J Control Release 2005;108:460–71.
17. Qian W, Van Houten B. Alterations in bioenergetics due to changes in mitochondrial DNA copy number. Methods 2010;51:452–7.
18. Semenza GL. HIF-1 mediates the Warburg effect in clear cell renal carcinoma. J Bioenerg Biomembr 2007;39:231–4.
19. Yee Koh M, Spivak-Kroizman TR, Powis G. HIF-1 regulation: not so easy come, easy go. Trends Biochem Sci 2008;33:526–34.
20. Gevers W, Krebs HA. The effects of adenine nucleotides on carbohydrate metabolism in pigeon-liver homogenates. Biochem J 1966;98:720–35.
21. Ganapathy-Kanniappan S, Vali M, Kunjithapatham R, Buijs M, Syed LH, Rao PP, et al. 3-bromopyruvate: a new targeted antiglycolytic agent and a promise for cancer therapy. Curr Pharm Biotechnol 2010;11:510–7.
22. De Feo P, Di Loreto C, Lucidi P, Murdolo G, Parlanti N, De Cicco A, et al. Metabolic response to exercise. J Endocrinol Invest 2003;26:851–4.
23. Wells GD, Selvadurai H, Tein I. Bioenergetic provision of energy for muscular activity. Paediatr Respir Rev 2009;10:83–90.
24. Warburg O. Tests on surviving carcinoma cultures. Biochem Z 1923;142:317–33.
25. DeBerardinis RJ, Lum JJ, Hatzivassiliou G, Thompson CB. The biology of cancer: metabolic reprogramming fuels cell growth and proliferation. Cell Metab 2008;7:11–20.
26. Seyfried TN, Shelton LM. Cancer as a metabolic disease. Nutr Metab (Lond) 2010;7:7.
27. Thorn JA, Jarvis SM. Adenosine transporters. Gen Pharmacol 1996;27:613–20.

28. Trincavelli ML, Daniele S, Martini C. Adenosine receptors: what we know and what we are learning. Curr Top Med Chem 2010;10: 860–77.
29. Dvoriantchikova G, Barakat DJ, Hernandez E, Shestopalov VI, Ivanov D. Liposome-delivered ATP effectively protects the retina against ischemia-reperfusion injury. Mol Vis 2010;16:2882–90.
30. Hartner WC, Verma DD, Levchenko TS, Bernstein EA, Torchilin VP. ATP-loaded liposomes for treatment of myocardial ischemia. Wiley Interdiscip Rev Nanomed Nanobiotechnol 2009;1:530–9.
31. Liang W, Levchenko T, Khaw BA, Torchilin V. ATP-containing immunoliposomes specific for cardiac myosin. Curr Drug Deliv 2004;1:1–7.
32. Liang W, Levchenko TS, Torchilin VP. Encapsulation of ATP into liposomes by different methods: optimization of the procedure. J Microencapsul 2004;21:251–61.
33. Greijer AE, Delis-van Diemen PM, Fijneman RJ, Giles RH, Voest EE, van Hinsbergh VW, et al. Presence of HIF-1 and related genes in normal mucosa, adenomas and carcinomas of the colorectum. Virchows Arch 2008;452:535–44.
34. Tanaka H, Yamamoto M, Hashimoto N, Miyakoshi M, Tamakawa S, Yoshie M, et al. Hypoxia-independent overexpression of hypoxia-inducible factor 1alpha as an early change in mouse hepatocarcinogenesis. Cancer Res 2006;66:11263–70.
35. Zhong H, Semenza GL, Simons JW, De Marzo AM. Up-regulation of hypoxia-inducible factor 1alpha is an early event in prostate carcinogenesis. Cancer Detect Prev 2004;28:88–93.
36. Bos R, Zhong H, Hanrahan CF, Mommers EC, Semenza GL, Pinedo HM, et al. Levels of hypoxia-inducible factor-1 alpha during breast carcinogenesis. J Natl Cancer Inst 2001;93:309–14.
37. Elbers JR, Rijksen G, Staal GE, van Unnik JA, Roholl PJ, van Oirschot BA, et al. Activity of glycolytic enzymes and glucose-6-phosphate dehydrogenase in smooth muscle proliferation. Tumour Biol 1990;11: 210–9.
38. Mayer A, Hockel M, Wree A, Leo C, Horn LC, Vaupel P. Lack of hypoxic response in uterine leiomyomas despite severe tissue hypoxia. Cancer Res 2008;68:4719–26.
39. Okada K, Osaki M, Araki K, Ishiguro K, Ito H, Ohgi S. Expression of hypoxia-inducible factor (HIF-1alpha), VEGF-C and VEGF-D in non-invasive and invasive breast ductal carcinomas. Anticancer Res 2005;25:3003–9.
40. Vordermark D, Kraft P, Katzer A, Bolling T, Willner J, Flentje M. Glucose requirement for hypoxic accumulation of hypoxia-inducible factor-1alpha (HIF-1alpha). Cancer Lett 2005;230:122–33.
41. Fang M, Shen Z, Huang S, Zhao L, Chen S, Mak TW, et al. The ER UDPase ENTPD5 promotes protein N-glycosylation, the Warburg effect, and proliferation in the PTEN pathway. Cell 2011;143:711–24.